The Ligand Specificity of Yeast Rad53 FHA Domains at the +3 Position Is Determined by Nonconserved Residues[†,‡]

Suganya Yongkiettrakul,[§] In-Ja L. Byeon,[§,||] and Ming-Daw Tsai*[,§,⊥]

Ohio State Biochemistry Program, Department of Biochemistry, Department of Chemistry, and Campus Chemical Instrument Center, The Ohio State University, Columbus, Ohio 43210

Received December 6, 2003; Revised Manuscript Received January 29, 2004

ABSTRACT: On the basis of the results from our laboratory and others, we recently suggested that the ligand specificity of forkhead-associated (FHA) domains is controlled by variations in three major factors: (i) residues interacting with pThr, (ii) residues recognizing the +1 to +3 residues from pThr, and (iii) an extended binding surface. While the first factor has been well established by several solution and crystal structures of FHA−phosphopeptide complexes, the structural bases of the second and third factors are not well understood and are likely to vary greatly between different FHA domains. In this work, we proposed and tested the hypothesis that nonconserved residues G133 and G135 of FHA1 and I681 and D683 of FHA2, located outside of the core FHA region of yeast Rad53 FHA domains, contribute to the specific recognition of the +3 position of different phosphopeptides. By rational mutagenesis of these residues, the specificity of FHA1 has been changed from predominantly pTXXD to be equally acceptable for pTXXD, pTXXL, and pYXL, which are similar to the specificities of the FHA2 domain of Rad53. Conversely, the +3 position specificity of FHA2 has been engineered to be more like FHA1 with the I681A mutation. These results were based on library screening as well as binding analyses of specific phosphopeptides. Furthermore, results of structural analyses by NMR indicate that some of these residues are also important for the structural integrity of the loops.

Recently, a phosphorylation-dependent recognition domain, known as the forkhead-associated (FHA)[1] domain, has been shown to mediate protein−protein interactions in many cellular processes of different species (*1*−*4*). Although the FHA domain has been found in more than 200 different proteins, the tertiary structure has only been obtained for yeast Rad53 (which consists of two FHA domains, FHA1 at the N-terminus and FHA2 at the C-terminus), human Chk2, human Chfr, human Ki67, and plant kinase-associated protein phosphatase (KAPP) (*5*−*11*). While the level of sequence homology of FHA domains is relatively low (∼20%), the tertiary structures reveal a remarkably similar folding, consisting of β-strands linked by several loops to form two large twisted antiparallel β-sheets folded into a β-sandwich.

The biological functions of FHA domains are very diverse. Therefore, the structure−function relationship of FHA domains and the structural basis of interactions between FHA domains and their binding proteins have been subjects of extensive research in many laboratories. The biological binding protein and the actual binding site have been unequivocally identified in only very few cases (*12*−*16*). Nevertheless, a wealth of information about the ligand specificity of FHA domains has been obtained by use of short phosphopeptides and phosphopeptide libraries consisting of 6−15 residues (*5*−*7*, *9*, *17*−*20*). These studies with short phosphopeptides showed that, while the Rad53 FHA1 domain specifically recognizes the phosphothreonine peptides containing Asp at the +3 position (pTXXD), the Rad53 FHA2 domain is able to bind both Thr- and Tyr-phosphorylated peptides containing a hydrophobic amino acid at the +3 and +2 positions (pTXXL/I and pYXL/I), respectively (*5*−*7*, *17*−*20*). In addition, it has been shown that the pTXXI motif is the consensus motif for human Chk2 FHA domain recognition (*9*). Interestingly, we recently showed that, unlike other FHA domains, the ligand recognition by the human Ki67 FHA domain is not dictated by any of the conserved motifs mentioned above, but involves an extended binding surface (*11*). These results indicate that, unlike other signal transduction domains that often recognize a specific binding motif (*21*, *22*), FHA domains from different proteins appear to show very diverse recognition mechanisms which could possibly be responsible for their diverse biological functions.

[†] This work was supported by NIH Grant CA87031 to M.-D.T. and by a fellowship from the Thailand Government to S.Y.

[‡] M.-D.T. dedicates this paper to Professor Heinz G. Floss on the occasion of his 70th birthday.

* To whom correspondence should be addressed: Department of Chemistry, The Ohio State University, 100 West 18th Ave., Columbus, OH 43210. E-mail: Tsai.7@osu.edu. Telephone: (614) 292-3080. Fax: (614) 292-1532.

[§] Ohio State Biochemistry Program.

[||] Current address: National Institute of Diabetes and Digestive and Kidney Diseases, National Institutes of Health, Bethesda, MD 20892.

[⊥] Department of Biochemistry, Department of Chemistry, and Campus Chemical Instrument Center.

[1] Abbreviations: DTT, 1,4-dithio-D,L-threitol; EDTA, ethylenediaminetetraacetic acid; FHA, forkhead-associated; GST, glutathione *S*-transferase; HEPES, *N*-(2-hydroxyethyl)piperazine-*N*′-(2-ethanesulfonic acid); HSQC, heteronuclear single-quantum coherence; SPR, surface plasmon resonance; MALDI-TOF, matrix-assisted laser desorption ionization time-of-flight; pThr and pT, phosphothreonine; pTyr and pY, phosphotyrosine; WT, wild type.

10.1021/bi036195f CCC: $27.50
Published on Web 03/03/2004

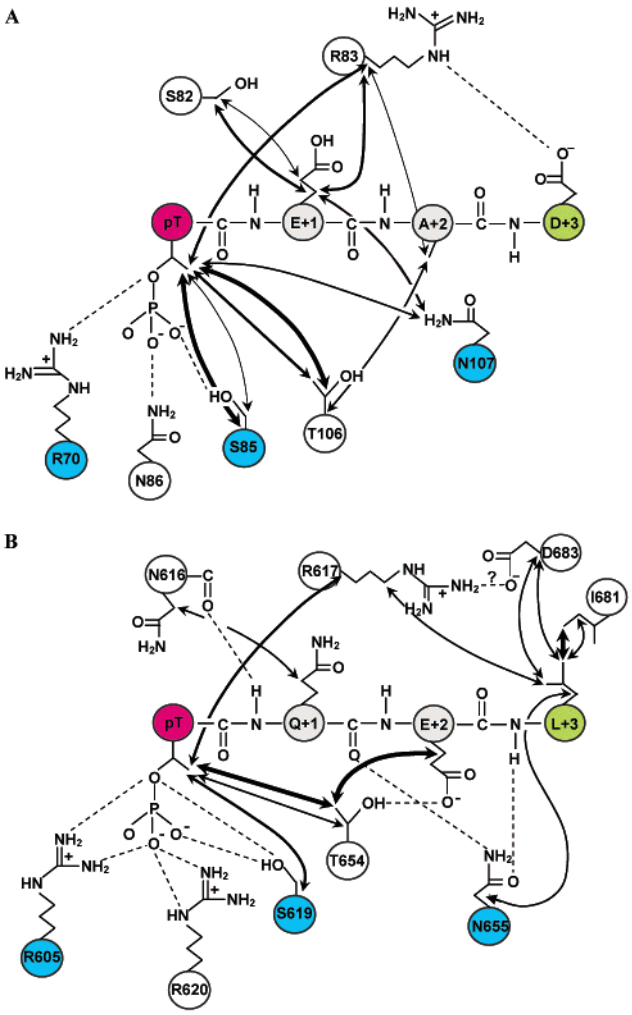

FIGURE 1: Diagrams showing detailed interactions between the phosphopeptide and the protein: (A) the FHA1−SLEV(pT)-EADATFVQ peptide complex (*7*) and (B) the FHA2−EVEL(pT)-QELP peptide complex from the NMR structure (*18*). Highly conserved residues are colored cyan. The possible H-bonding between the FHA domain and the peptide is shown with dashed lines, and intermolecular NOEs are represented as double-headed arrows, where thick, thin, and fine lines indicate strong, medium, and weak NOEs, respectively.

On the basis of these studies, we proposed that the ligand specificity of FHA domains is controlled by three major factors (residues interacting with pThr, residues recognizing the +1 to +3 positions of pT peptides, and an extended binding surface) and that variations in the relative roles of the three factors likely contribute to the diverse ligand specificity and diverse biological functions of FHA domains (*11*).

Although the results obtained with short phosphopeptides may not reveal the actual biological binding site, they give useful information for understanding the structural basis of FHA recognition. To this end, we have reported the solution structures of the complexes of FHA2 with a pT peptide [EVEL(pT)QELP] and a pY peptide [EDI(pY)YLD], and the solution structure of the complex of FHA1 with a pT peptide [SLEV(pT)EADATFVQ]. Another group has reported the crystal structure of the complex of FHA1 with another pT peptide [SLEV(pT)EADATFAKK] (*6*). Analyses of these structures, as shown in Figure 1, indicate that binding of the pThr residue involves primarily conserved residues R70 and S85 and a nonconserved N86 of FHA1 (or R605, S619, and R620, respectively, of FHA2). The roles of these residues in the recognition of the pThr residue have been supported by the results of site-directed mutagenesis (*5*, *6*).

This paper focuses on how the FHA domains of Rad53 specifically recognize distinct pT+3 residues. The goal is to use the approach of site-directed mutagenesis to make FHA1 show FHA2-like specificity and vice versa. The results indicate that single-point mutation of nonconserved residues residing outside the core region at the C-terminus could change the binding specificity of the protein. Furthermore, structural analyses of the mutants suggested that some of these nonconserved residues also contribute to maintaining the right orientation of peptide-binding loops.

MATERIALS AND METHODS

Materials. The pT and pY peptides used in this study were Rad9-derived peptides, synthesized by Genemed Synthesis, Inc. (South San Francisco, CA). All other chemicals were obtained from Aldrich Chemical unless stated otherwise.

Site-Directed Mutagenesis of FHA1 and FHA2 Domains. The pET29a(+) vector (Novagen) containing the genes encoding the FHA1 domain (residues 14−164) and the FHA2 domain (residues 573−730) of Rad53 with GST fusion at the N-terminus were used as a template for generating single mutants [GST−FHA1(G133I), GST−FHA1(G135D), GST−FHA2(I681A), and GST−FHA2(D683A)] and double mutants [GST−FHA1(G133I/G135D) and GST−FHA2(I681A/D683A)]. Mutagenesis was performed by using the Quick Change site-directed mutagenesis kit (Stratagene). The sequence of mutagenic forward primers, with base substitutions underlined, used for generating each mutant are listed here: FHA1(G133I), 5′-GAAATAACCGTTATCGTAG-GCGTGGAA-3′; FHA1(G135D), 5′-ACCGTTGGTGTA-GATGTGGAATCAG-3′; FHA1(G133I/G135D), 5′-GA-AATAACCGTTATCGTAGACGTGGAATCAG-3′; FHA2-(I681A), 5′-GAAATCAAGATCGCATGGGATAAAAACA-3′; FHA2(D683A), 5′-CAAGATCATTTGGGCAAAAAA-CAATAAA-3′; and FHA2(I681A/D683A), 5′-GAAATC-AAGATCGCATGGGCAAAAAACAATA-3′. DNA sequences were subsequently verified with a 3700 DNA analyzer (Applied Biosystems, Inc.).

Protein Expression and Purification. The ^{15}N-labeled GST fusion proteins of the mutants were expressed in *Escherichia coli* BL21(DE3), using M9 medium containing $^{15}NH_4Cl$. The protein purification was performed using glutathione agarose (Sigma) followed by removal of the GST tag with thrombin (Sigma) digestion. Subsequently, the proteins were purified by S-100 gel filtration chromatography. The protein samples were finally maintained in 10 mM phosphate buffer, 1 mM EDTA, and 5 mM DTT (pH 6.5). The purification was verified throughout by SDS−PAGE analysis. Protein concentrations were spectrophotometrically determined at 280 nm, using extinction coefficients of 12 660 and 15 220 M^{-1} cm^{-1} for FHA1 and FHA2 domains, respectively.

Analysis of Phosphopeptide Binding Affinity by Surface Plasmon Resonance. Binding analysis by SPR was performed on a BIAcore 3000 instrument at 25 °C. The peptides were first biotinylated, as previously described (*7*). The biotinylated peptides were then immobilized on a SA sensor chip, which had been pretreated and conditioned according to the

manufacturer's recommendations. The buffer used throughout the SPR experiment consisted of 10 mM phosphate and 1 mM EDTA (pH 7.4). Each peptide was immobilized at each channel with a flow rate 10 μL/min until a baseline increase of 80−200 resonance units (RU) was obtained. Subsequently, the chip was washed with 50 mM NaOH and 1 M NaCl to remove the nonspecific bound peptides. After the peptide immobilization, a protein solution with an increasing concentration was passed through the chip with a flow rate of 10 μL/min for 4 min. The chip surface was regenerated with 50 mM NaOH and 1 M NaCl after each individual measurement to obtain the original baseline for subsequent measurements. As a consequence of the protein binding to the peptide, the RU changes with time, providing the sensorgram. At the equilibrium stage of the sensorgram, the absolute RU changes at each protein concentration were recorded and used for calculating the dissociation constants (K_d).

Analysis of Phosphopeptide Binding Affinity by NMR. NMR experiments were performed on a Bruker DMX-600 spectrometer at 20 °C. The samples contained 10 mM phosphate buffer, 1 mM EDTA, and 5 mM DTT in a 95% H_2O/5% ^2H_2O mixture at pH 6.5. The protein concentration used in the experiment was 0.3−0.6 mM. Peptide binding experiments were conducted by recording a series of two-dimensional (2D) ^{15}N HSQC spectra for uniformly ^{15}N-labeled samples with different peptide concentrations at pH 6.5. The dissociation constants (K_d) were calculated by assuming single-site binding and a fast exchange regime, as described previously (*18*, *23*).

pT Peptide Library Screening. A ladder pT peptide library [AXX(pT)XXXXABBRM-resin] was used in this study. Purified FHA1(WT), FHA1(G135D), FHA2(WT), and FHA2-(I681A) proteins were biotinylated with sulfo-NHS-biotin as described by the manufacturer. The screening of biotinylated wild-type FHA1 (0.1 μM) and FHA2 (1.0 μM), as positive controls, was conducted with 60 mg of TentaGel beads containing pT peptide libraries. Screening of FHA1-(G135D) was performed with 60 mg of beads and 20 μM biotinylated protein. For the screening of FHA2(I681A), the experiment was carried out with 40 mg of bead and 50 μM biotinylated protein. The details of the screening procedure were similar to those in the previous study (*7*). Positive blue beads were selected from the library screening. Peptides were then removed from the beads and subjected to amino acid sequencing by a MALDI-TOF mass spectrometer (Reflex III, Bruker Daltonics). The negative control in which the reaction was conducted without the biotinylated protein yielded colorless beads only.

RESULTS AND DISCUSSION

Hypothesis: Nonconserved Residues Are Involved in pT+3 Recognition. The residue likely to be responsible for the preference of D at the pT+3 position by FHA1 is R83 which forms a salt bridge with the side chain of D at the pT+3 position as shown in Figure 1. A possible strategy for changing the specificity of FHA1 is to substitute R83 with a different residue. However, the corresponding residue is also an arginine (R617) in FHA2. Thus, a different strategy was used to change the specificity of FHA1 to be FHA2-like. As illustrated in Figure 2, detailed analysis of the structures indicated that the corresponding residue, R617, possibly forms a salt bridge with D683 in FHA2. The residue corresponding to D683 is G135 in FHA1. Thus, we hypothesized that changing G135 to D could create a salt bridge between R83 and D135, thus inhibiting the ability of R83 to interact with a D at the pT+3 position. Conversely, changing D683 to A could free up the side chain of R617 and force FHA2 to prefer a D at the pT+3 position. Likewise, we hypothesized that changing G133 to I could make FHA1 more likely to accept a hydrophobic residue at the pT+3 position, and changing I681 to A could reduce the preference of FHA2 for a hydrophobic residue at the pT+3 position. Therefore, we decided to construct G133I, G135D, I681A, D683A, and double mutants G133I/G135D and I681A/D683A. Note that these four residues are all nonconserved residues located at the loops connecting the β-strands.

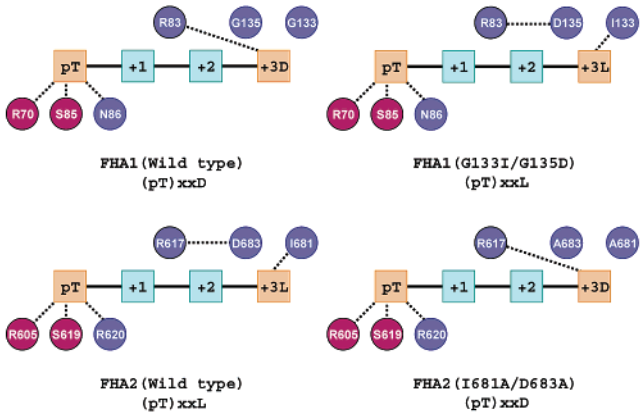

FIGURE 2: Diagrams illustrating our hypotheses about the roles of nonconserved residues and the possible effects of mutations of these residues. Highly conserved residues and nonconserved residues are colored dark red and purple, respectively. The dotted lines represent the interactions between the pT peptide and the protein.

Loop Conformations Are Perturbed in the Mutants. We first examined the possible structural roles of the four nonconserved residues: G133, G135, I681, and D683. All mutants were expressed as soluble GST fusion proteins followed by removal of the GST tag. It was found that two of the mutants, FHA2(D683A) and FHA2(I681A/D683A), precipitated nearly completely after removal of the GST tag. This result suggests, indirectly, that the R617−D683 salt bridge between the β3′−β4 loop and the β9−β10 loop is involved in the stabilization of the structure of FHA2.

The four remaining mutant proteins could be purified in the soluble form. However, significant precipitation was also observed for FHA1(G133I). Since G133 is located in the initial part of the loop formed by the β9−β10 strands, the introduction of a bulky group in the G133I mutant possibly affects the local conformation of the β9−β10 loop and exposes the hydrophobic residue isoleucine, resulting in the protein precipitation. Less protein precipitation was observed in the FHA1(G133I/G135D) double mutant, possibly due to compensation for the effect of the G133I mutation by the G135D mutation. In support of this interpretation, it was found that the G135D single mutant exhibited enhanced protein stability and solubility, as no protein precipitation was observed throughout the purification.

The four mutants that could be obtained in the soluble form were further characterized by ^{15}N HSQC NMR experiments. Figure 3 shows the superposition of the spectra of

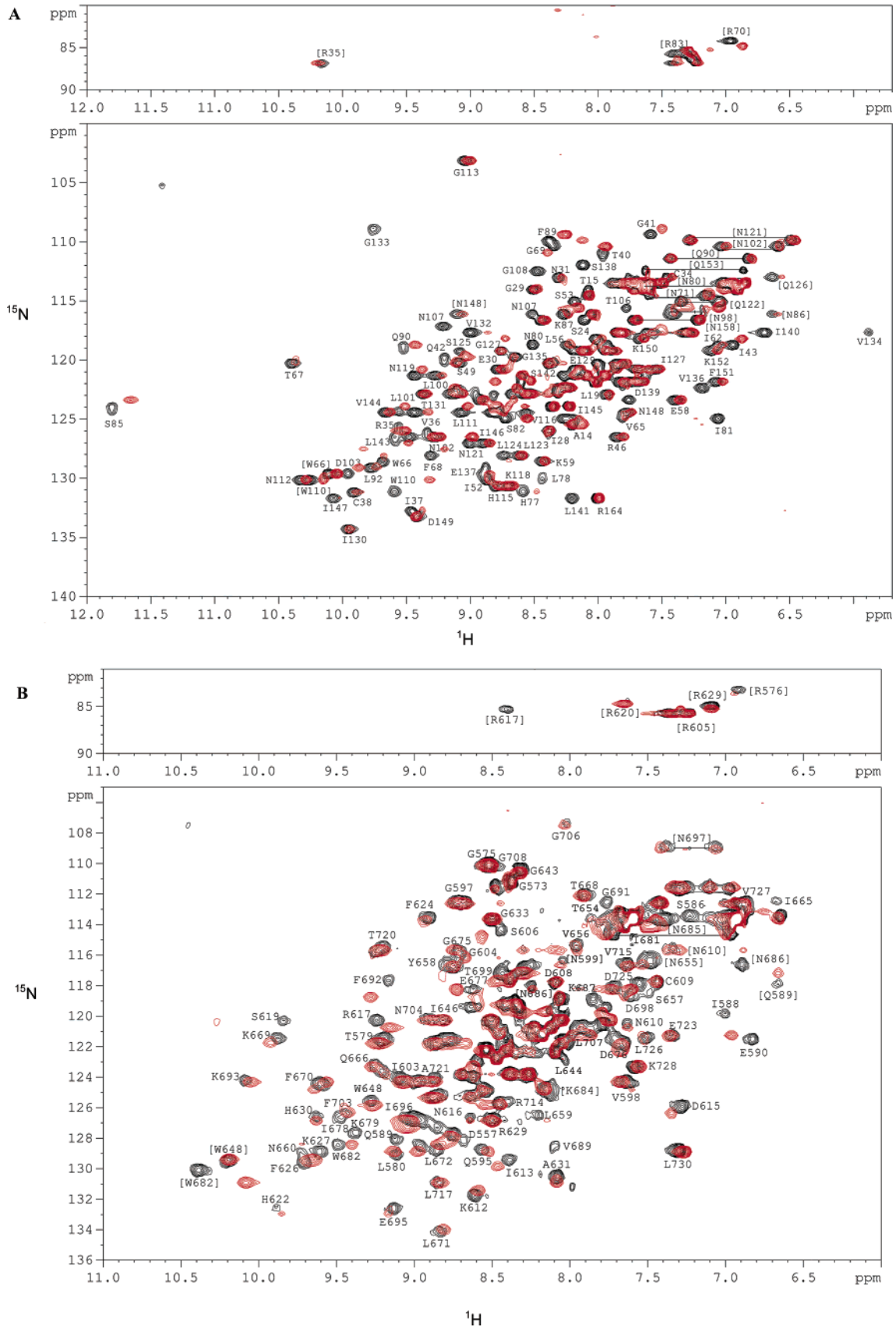

FIGURE 3: Comparison between ^{15}N HSQC spectra of the wild type and mutants. (A) Wild-type FHA1 domain (black) and mutant G133I domain (red). (B) Wild-type FHA2 domain (black) and mutant I681A domain (red). The assignments in brackets are for side chains.

FHA1(WT) with G133I (panel A) and FHA2(WT) with I681A (panel B). The spectra of the other two mutants, G135D and G133I/G135D, are not shown. The assignments shown in the figure are based on previous assignments of the WT FHA domains (*5*, *7*, *18*, *19*). The peaks for the mutants were assigned on the basis of the visual comparison

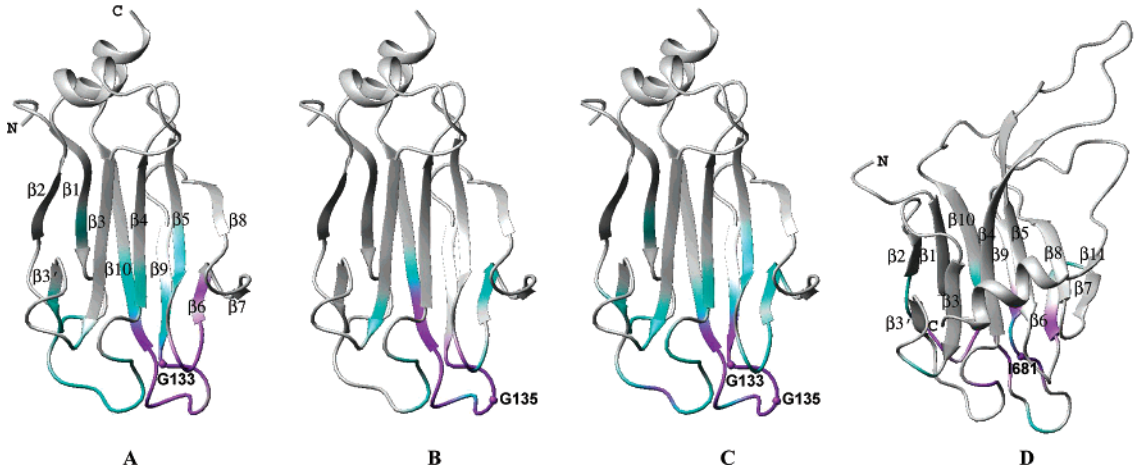

FIGURE 4: Ribbon diagrams of FHA1 and FHA2 domains showing the comparison of the effect of the (A) G133I, (B) G135D, (C) and G133I/G135D mutants of the FHA1 domain and (D) the I681A mutant of the FHA2 domain. The combined chemical shift changes due to the mutation were calculated according to the equation $\min\Delta\text{ppm} = [\Delta\delta_{HN}^2 + (\Delta\delta_N\alpha_N)^2]^{1/2}$, where $\Delta\delta_{HN}$ and $\Delta\delta_N$ are the ^{1}HN and ^{15}N chemical shift differences in parts per million, respectively, and α_N is the scaling factor used to normalize the ^{1}H and ^{15}N chemical shifts (0.17) (*26*). The residues are color-coded according to the degree of the combined chemical shift changes: gray if $\min\Delta\text{ppm} < 0.1$ ppm, turquoise if 0.1 ppm $< \min\Delta\text{ppm} <$ 0.3 ppm, and purple if $\min\Delta\text{ppm} > 0.3$ ppm. The mutated residues are represented as spheres. The structures were viewed with MolMol (*27*, *28*).

with the WT spectra. Overall, a large number of peaks are shifted in all four mutants. Consistent with the interpretations on the basis of precipitation of samples described above, G133I displayed the greatest perturbation in the HSQC spectrum, in which two-thirds of the peaks are shifted and 17 peaks disappear.

On the basis of the assignments and structures of wild-type FHA1 and FHA2, the residues with different degrees of chemical shift changes are shown in Figure 4 for all four mutants. As shown in Figure 4A, most of the residues of the FHA1(G133I) mutant with larger shifted resonances are located in $\beta3'-\beta4$, $\beta5-\beta6$, and $\beta9-\beta10$ loops, which are responsible for phosphopeptide binding. Some of the conserved residues involved in pTXXD peptide binding, R70, R83, S85, T106, and N107, are among the residues with the largest shifts. These results suggest that the G133I mutation likely perturbs the orientation of the loops involved in the phosphopeptide binding. Some of the residues in the β-strands are also perturbed, but only with small chemical shift changes. The pattern of chemical shift perturbation in the G133I/G135D double mutant is very similar to that of the G133I single mutant, as shown in Figure 4C. Smaller and less global changes were observed for G135D, but the residues with perturbed chemical shifts are also located mainly in the loops as shown in Figure 4B. For the FHA2(I681A) mutant, the degree of perturbations is smaller than that of the other three FHA1 mutants as shown in Figure 4D.

As we have advocated, the functional role of a mutated residue cannot be unequivocally assigned if the structure of the mutant protein is perturbed, since the effect of the function could be caused by structural perturbations (*24*). However, chemical shift changes are an overly sensitive indication of structural perturbations. It is possible that the structural perturbations in the mutants are not sufficient to cause unpredicted functional changes. Thus, we proceeded to study the functional properties of the mutants as described in the following sections.

Library Screening Indicates Changes in Ligand Specificity. We first used the library screening approach to examine, qualitatively, whether the designed mutations led to changes in ligand specificity. The pT peptide library [AXX(pT)-XXXX] was used, and the experiment was performed as previously described (*7*). Wild-type FHA1 and FHA2 domains were used as controls in this study. As shown in Figure 5A, the results clearly show that, in agreement with previous reports (*7*), the wild-type FHA1 domain prefers the pT peptide containing D/E at the +3 position (75% abundance). On the other hand, the G135D mutation led a significantly reduced preference of D/E at the +3 position. This result indicates that G135 is one of the determinant residues for FHA1 specificity, and supports the hypothesis illustrated in Figure 2 that changing G135 to D could lead to a salt bridge between R83 and D135, thus inhibiting the ability of R83 to interact with a D at the pT+3 position.

So far, the preference at the pT+4 position of the FHA domain has never been tested. In this study, the use of a pT peptide library containing random residues at the pT+4 position allowed us to examine the preference of FHA1 at the pT+4 position of the phosphopeptide. The result in Figure 5B shows that there was not a certain residue predominantly selected at the pT+4 position from the screening of either wild-type or mutant FHA1. This evidence suggests that the pT+4 residue may not contribute to the specific interaction between FHA1 and the pT peptide.

Although the results of library screening for G135D support our hypothesis, it took a very high concentration of the mutant proteins to obtain blue beads, possibly due to the loss of clear preferences for specific sequences. Furthermore, such results are only qualitative. In addition to FHA1(G135D), we also screened FHA2(I681A) against the same pT peptide library but were unable to obtain blue beads even at a very high concentration of the mutant protein (50 μM). Again, this observation indirectly supports the importance of I681 in the recognition of ligands, but it is based on negative results. We therefore did not perform further library screening but turned to quantitative binding analyses as described in the next section.

NMR and SPR Analyses of Binding of Phosphopeptide to the Mutants. Three phosphopeptides were used to examine

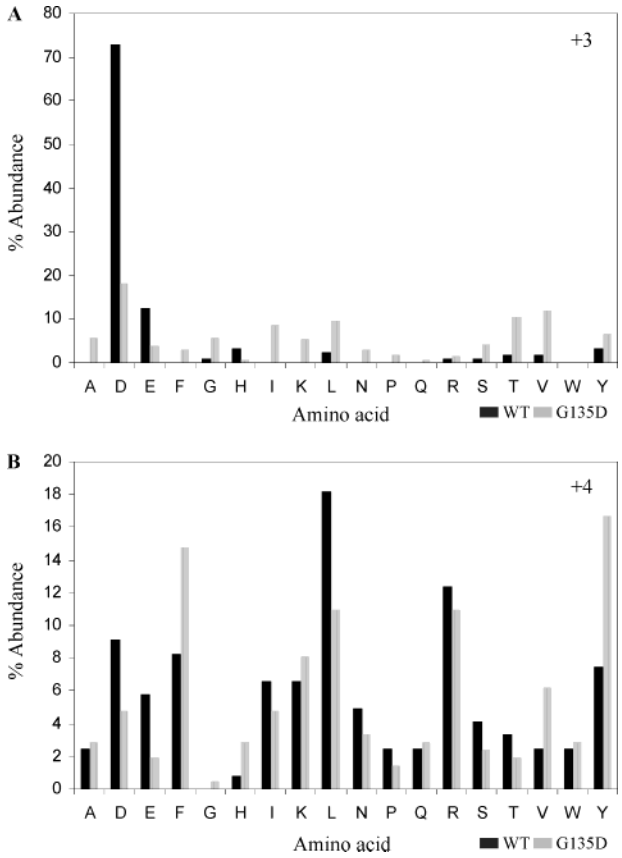

FIGURE 5: Preference for an amino acid at (A) the +3 position and (B) the +4 position relative to the pT residue observed from the screening of FHA1(WT) and FHA1(G135D) against the AXX-(pT)XXXX peptide library. The percent abundance is the percent appearance of each residue at the randomized position.

the affinities of the four FHA mutants for phosphopeptides: SLEV(pT)EADATFVQ (peptide I), EVEL(pT)QELP (peptide II), and EDI(pY)YLD (peptide III, a phosphotyrosine peptide). All three phosphopeptides correspond to partial sequences of Rad9, a potential binding partner of the FHA1 and FHA2 domains (*7*, *18*, *19*). The structures of the FHA1−peptide I, FHA2−peptide II, and FHA2−peptide III complexes have all been determined by NMR in our laboratory, and their binding properties have been characterized (*7*, *18*−*20*). Thus, these phosphopeptides serve as good systems for examining the properties of the mutants.

The binding properties of all four mutants toward all three peptides were studied by ^{15}N HSQC titration experiments. Dissociation constants (K_d) were measured from the NMR experiments in the cases of weaker binding (fast exchange on the NMR time scale). When the binding was strong and the free and bound species were in slow exchange on the NMR time scale, the K_d was determined by surface plasmon resonance (SPR) experiments. Both methods have been used previously for FHA domains. The dissociation constants are summarized in Table 1.

Analyses of the results of ^{15}N HSQC titration experiments indicated that many peaks corresponding to amino acids in the peptide binding regions undergo significant chemical shift changes upon addition of increasing concentrations of phosphopeptides. Peaks corresponding to R70, R83, and S85 displayed the greatest shifts. The chemical shift changes caused by addition of phosphopeptides are illustrated by the NH cross-peak of a single residue, S85 of FHA1 (Figure 6) and S619 of FHA2 (Figure 7). This conserved serine residue has been suggested to directly interact with the pThr residue of the phosphopeptide (*6*, *18*−*20*). Its NH cross-peak is located in a distinct position in the ^{15}N HSQC spectra and is very sensitive to mutagenesis as shown in Figure 3. Binding of an FHA domain to a phosphopeptide almost always causes shifts of this cross-peak (*18*−*20*).

It is of interest to mention that binding of phosphopeptides can also change the dynamic property of the mutants. For example, some of the weak and invisible cross-peaks in the ^{15}N HSQC spectrum of the FHA1(G133I) mutant became strong and visible upon titration with the SLEV(pT)-EADATFVQ phosphopeptide (spectra not shown).

Changes in the Ligand Specificity of the Mutants. As shown in Table 1, the ligand specificities of wild-type FHA1 and FHA2 differ significantly, in agreement with previous reports (*5*, *7*, *18*). FHA1 binds peptide I (pTXXD) tightly (K_d = 0.4 μM) and peptide II (pTXXL) weakly (K_d = 149 μM) and does not bind peptide III (pYXL), whereas FHA2 binds the three phosphopeptides in the following order of affinity: peptide II (K_d = 13 μM) > peptide III (K_d = 100 μM) > peptide I (K_d = 335 μM). As we have anticipated, the two single mutants and one double mutant of the FHA1 domain all bind peptide II and peptide III with K_d values comparable to those of FHA2. The affinities of these three mutants for peptide I have also decreased by a factor of 5−25, though not abolished. These results support our hypotheses that changing G135 to D could lead to a salt bridge between R83 and D135, thus inhibiting the ability of R83 to interact with a D at the pT+3 position, and that changing G133 to isoleucine could make FHA1 more likely to accept a hydrophobic residue at the pT+3 position.

The results in Table 1 also show that the I681A mutation of the FHA2 domain significantly weakened the pTXXL peptide binding affinity, as evidenced by an increase in the K_d for peptide II from 13 to 165 μM. There is little change in the binding affinity toward peptides I and III. This result again supports an important role of I681 in the specific interaction between the FHA2 domain and the EVEL(pT)-QELP peptide, and the hypothesis that elimination of the hydrophobic side chain of I681 could lead to decrease in the strength of the FHA2−EVEL(pT)QELP interaction.

Taken together, our structural and functional analyses indicate that, despite the substantial perturbation in the conformation of the mutants, it is possible to change the ligand specificity, making FHA1 more like FHA2 and vice versa. Thus, these nonconserved residues appear to play both structural and functional roles.

Comparison with Other FHA Domains. Overall, the results described in this paper provide further insight into the functional diversity of FHA domains. As we have proposed recently, three major factors contribute to the ligand specificity of FHA domains. The recognition of the pThr residue is contributed mainly by conserved residues in the $\beta 3'-\beta 4$ loop of Rad53 FHA domains. The nonconserved residues mentioned in this work, which vary for different FHA domains, contribute to the recognition of pT+3 residues. The third factor is an extended binding surface observed for Ki67 FHA (*11*). It remains to be established whether the third factor is unique to Ki67 or also exists for other FHA domains.

Variations in the structural basis of pT+3 recognition are further illustrated by comparing the structures of FHA−

Table 1: Dissociation Constants for Phosphopeptide Binding of Wild-Type and Mutant FHA Domains

	K_d (μM)					
	FHA1 domain				FHA2 domain	
phosphopeptide	WT	G133I	G135D	G133I/G135D	WT	I681A
(I) SLEV(pT)EADATFVQ	0.41 ± 0.12[a]	2.70 ± 0.58[a]	10.49 ± 1.37[a]	2.69 ± 0.20[a]	335[b]	138
(II) EVEL(pT)QELP	149	20	15	28	13[b]	165
(III) EDI(pY)YLD	nd[d]	73	202	120	100[c]	266

[a] Data obtained by SPR analyses; the rest of the data were obtained from NMR analyses. [b] Data obtained from ref *18*. [c] Data obtained from ref *5*. [d] Not detected.

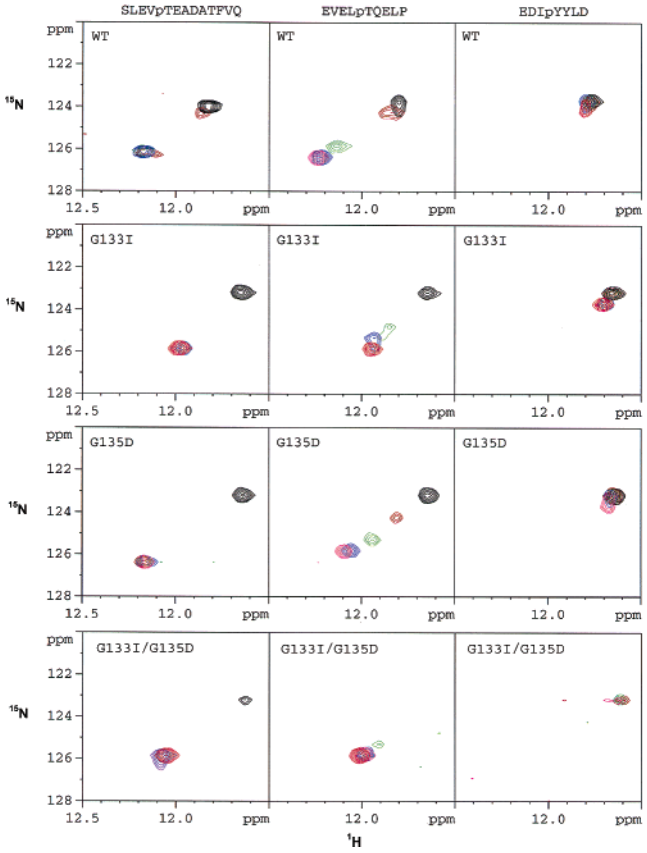

FIGURE 6: Chemical shift change of the backbone amide group of S85 of the FHA1 domain observed from ^{15}N HSQC spectra upon peptide titration at peptide-to-protein ratios of 0 (black), 0.5 (brown), 1 (green), 2 (blue), 4 (pink), and 8 (red).

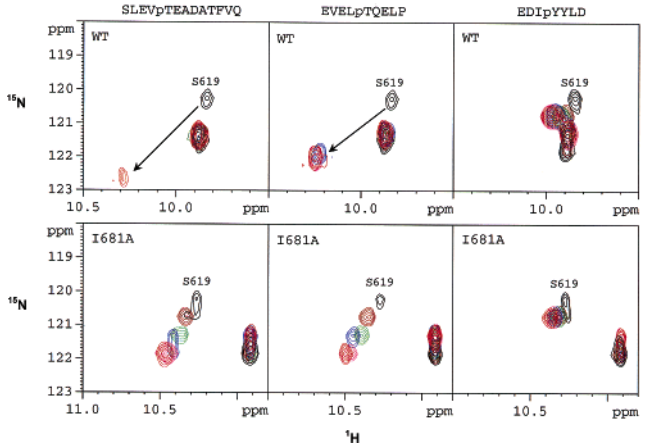

FIGURE 7: Chemical shift change of the backbone amide group of S619 of the FHA2 domain observed from ^{15}N HSQC spectra upon peptide titration at peptide-to-protein ratios of 0 (black), 0.5 (brown), 1 (green), 2 (blue), 4 (pink), and 8 (red). The arrows indicate the direction of chemical shift change.

phosphopeptide complexes reported to date: FHA1 and FHA2 of Rad53, human Chk2 FHA, and human Ki67 FHA (*6*, *9*, *11*, *18*−*20*). Like Rad53 FHA2, human Chk2 FHA specifically recognizes a hydrophobic residue at the +3 position of pT peptides. However, the specific determinant for the +3 recognition differs between these two cases. Whereas the specific pT+3 recognition of FHA2 is mainly determined by a nonconserved I681 located in the β9−β10 loop, the specific recognition of Chk2 for hydrophobic residues at the pT+3 position is determined by a shallow pocket on the protein surface (*9*). For Ki67 FHA, there is a leucine, I90, which corresponds to I681 of Rad53 FHA2 on the basis of structure-based alignments. However, the Ki67 FHA domain does not specifically recognize hydrophobic residues at the pT+3 position. Understanding this difference must await the availability of the structure of the Ki67 FHA complex with its binding partner; so far, only qualitative structural analyses of the complex have been reported (*11*).

Conclusion. Of the many protein domains involved in signal transduction, the FHA domain is one that has demonstrated great functional diversity. Understanding the structural basis of this functional diversity will be very important in understanding the mechanism of signal transduction. Our laboratory has been working toward this goal by reporting structure−function relationships of Rad53 FHA1, Rad53 FHA2, Ki67 FHA, and Chk2 FHA (*5*, *7*, *11*, *18*−*20*, *25*). In this work, we have moved another important step in this direction by examining the structural basis of the recognition of the pT+3 residue by FHA1 and FHA2 of Rad53.

ACKNOWLEDGMENT

We thank Dr. Yong Ju and Yu Wang for the synthesis of the pT peptide library, Dr. Chunhua Yuan for advice in performing NMR experiments and for valuable discussion, and Erica Waite for technical assistance in library screening.

REFERENCES

1. Hofmann, K., and Bucher, P. (1995) The FHA domain: a putative nuclear signalling domain found in protein kinases and transcription factors, *Trends Biochem. Sci. 20*, 347−349.
2. Durocher, D., and Jackson, S. P. (2002) The FHA domain, *FEBS Lett. 513*, 58−66.
3. Pallen, M., Chaudhuri, R., and Khan, A. (2002) Bacterial FHA domains: neglected players in the phospho-threonine signalling game? *Trends Microbiol. 10*, 556−563.
4. Li, J., Lee, G. I., Van Doren, S. R., and Walker, J. C. (2000) The FHA domain mediates phosphoprotein interactions, *J. Cell Sci. 113* (Part 23), 4143−4149.
5. Liao, H., Byeon, I. J., and Tsai, M. D. (1999) Structure and function of a new phosphopeptide-binding domain containing the FHA2 of Rad53, *J. Mol. Biol. 294*, 1041−1049.

6. Durocher, D., Taylor, I. A., Sarbassova, D., Haire, L. F., Westcott, S. L., Jackson, S. P., Smerdon, S. J., and Yaffe, M. B. (2000) The molecular basis of FHA domain:phosphopeptide binding specificity and implications for phospho-dependent signaling mechanisms, *Mol. Cell 6*, 1169−1182.
7. Liao, H., Yuan, C., Su, M. I., Yongkiettrakul, S., Qin, D., Li, H., Byeon, I. J., Pei, D., and Tsai, M. D. (2000) Structure of the FHA1 domain of yeast Rad53 and identification of binding sites for both FHA1 and its target protein Rad9, *J. Mol. Biol. 304*, 941−951.
8. Stavridi, E. S., Huyen, Y., Loreto, I. R., Scolnick, D. M., Halazonetis, T. D., Pavletich, N. P., and Jeffrey, P. D. (2002) Crystal structure of the FHA domain of the Chfr mitotic checkpoint protein and its complex with tungstate, *Structure 10*, 891−899.
9. Li, J., Williams, B. L., Haire, L. F., Goldberg, M., Wilker, E., Durocher, D., Yaffe, M. B., Jackson, S. P., and Smerdon, S. J. (2002) Structural and functional versatility of the FHA domain in DNA-damage signaling by the tumor suppressor kinase Chk2, *Mol. Cell 9*, 1045−1054.
10. Lee, G. I., Ding, Z., Walker, J. C., and Van Doren, S. R. (2003) NMR structure of the forkhead-associated domain from the *Arabidopsis* receptor kinase-associated protein phosphatase, *Proc. Natl. Acad. Sci. U.S.A. 100*, 11261−11266.
11. Li, H., Byeon, I.-J., Ju, Y., and Tsai, M.-D. (2004) Structure of human Ki67 FHA domain and its binding to a phosphoprotein fragment from hNIFK reveal unique recognition sites and new views to the structural basis of FHA domain functions, *J. Mol. Biol. 335*, 371−381.
12. Schwartz, M. F., Duong, J. K., Sun, Z., Morrow, J. S., Pradhan, D., and Stern, D. F. (2002) Rad9 phosphorylation sites couple Rad53 to the *Saccharomyces cerevisiae* DNA damage checkpoint, *Mol. Cell 9*, 1055−1065.
13. Sun, Z., Hsiao, J., Fay, D. S., and Stern, D. F. (1998) Rad53 FHA domain associated with phosphorylated Rad9 in the DNA damage checkpoint, *Science 281*, 272−274.
14. Takagi, M., Sueishi, M., Saiwaki, T., Kametaka, A., and Yoneda, Y. (2001) A novel nucleolar protein, NIFK, interacts with the forkhead associated domain of Ki-67 antigen in mitosis, *J. Biol. Chem. 276*, 25386−25391.
15. Sueishi, M., Takagi, M., and Yoneda, Y. (2000) The forkhead-associated domain of Ki-67 antigen interacts with the novel kinesin-like protein Hklp2, *J. Biol. Chem. 275*, 28888−28892.
16. Li, J., Smith, G. P., and Walker, J. C. (1999) Kinase interaction domain of kinase-associated protein phosphatase, a phosphoprotein-binding domain, *Proc. Natl. Acad. Sci. U.S.A. 96*, 7821−7826.
17. Durocher, D., Henckel, J., Fersht, A. R., and Jackson, S. P. (1999) The FHA domain is a modular phosphopeptide recognition motif, *Mol. Cell 4*, 387−394.
18. Byeon, I. J., Yongkiettrakul, S., and Tsai, M. D. (2001) Solution structure of the yeast Rad53 FHA2 complexed with a phosphothreonine peptide pTXXL: comparison with the structures of FHA2-pYXL and FHA1-pTXXD complexes, *J. Mol. Biol. 314*, 577−588.
19. Wang, P., Byeon, I. J., Liao, H., Beebe, K. D., Yongkiettrakul, S., Pei, D., and Tsai, M. D. (2000) Structure and specificity of the interaction between the FHA2 domain of Rad53 and phosphotyrosyl peptides, *J. Mol. Biol. 302*, 927−940.
20. Yuan, C., Yongkiettrakul, S., Byeon, I. J., Zhou, S., and Tsai, M. D. (2001) Solution structures of two FHA1-phosphothreonine peptide complexes provide insight into the structural basis of the ligand specificity of FHA1 from yeast Rad53, *J. Mol. Biol. 314*, 563−575.
21. Pawson, T. (2002) Regulation and targets of receptor tyrosine kinases, *Eur. J. Cancer 38* (Suppl. 5), S3−S10.
22. Pawson, T., and Nash, P. (2000) Protein−protein interactions define specificity in signal transduction, *Genes Dev. 14*, 1027−1047.
23. De Macro, A., Petros, A. M., Lausen, R. A., and Linás, M. (1987) Analysis of ligand-binding to the kringle 4 fragment from human plasminogen, *Eur. Biophys. J. 14*, 359−368.
24. Tsai, M. D., and Yan, H. G. (1991) Mechanism of adenylate kinase: site-directed mutagenesis versus X-ray and NMR, *Biochemistry 30*, 6806−6818.
25. Qin, D., Lee, H., Yuan, C., Ju, Y., and Tsai, M. D. (2003) Identification of potential binding sites for the FHA domain of human Chk2 by in vitro binding studies, *Biochem. Biophys. Res. Commun. 311*, 803−808.
26. Farmer, B. T., II, Constantine, K. L., Goldfarb, V., Friedrichs, M. S., Wittekind, M., Yanchunas, J., Jr., Robertson, J. G., and Mueller, L. (1996) Localizing the $NADP^+$ binding site on the MurB enzyme by NMR, *Nat. Struct. Biol. 3*, 995−997.
27. Koradi, R., Billeter, M., and Wuthrich, K. (1996) MOLMOL: a program for display and analysis of macromolecular structures, *J. Mol. Graph. 14*, 51−55.
28. Koradi, R., Billeter, M., and Wuthrich, K. (1996) MOLMOL: a program for display and analysis of macromolecular structures, *J. Mol. Graph. 14*, 29−32.

BI036195F